Int. J. Electrochem. Sci., 11 **(2016)** 5403 – 5415, doi: 10.20964/2016.07.65

International Journal of
ELECTROCHEMICAL
SCIENCE
www.electrochemsci.org

Experimental Research on Multiple Wire Electrode Electrochemical Micro Machining

K. Xu[1], *Y.B. Zeng*[1,2,*], *P. Li*[1], *X.L. Fang*[1], *D. Zhu*[1,2]

[1] College of Mechanical and Electrical Engineering, Nanjing University of Aeronautics and Astronautics, Nanjing, China, 210016
[2] Jiangsu Key Laboratory of Precision and Micro-Manufacturing Technology, Nanjing, China, 210016
[*]E-mail: binyz@nuaa.edu.cn

Received: 7 April 2016 / *Accepted:* 15 May 2016 / *Published:* 4 June 2016

Wire electrochemical micro machining is potentially a useful method in the fabrication of metal micro parts or devices with high aspect ratios and high surface quality. However, because the material removal rate is slow, a long machining time is required to produce the micro products. To increase productivity, the use of multiple wire electrodes is introduced, and an electrochemical cell model of multiple wire electrodes built. It is proved theoretically and experimentally that the overall machining efficiency can be increased by using multiple wire electrodes, but that it does not increase linearly with the number of wire electrodes. To obtain the optimal pulse conditions for stable machining, changes in the average slit width and the uniformity of the slit width using three wire electrodes, according to the applied pulse voltage, pulse on-time, pulse period and feed rate, are investigated. Finally, with three wire electrodes, micro structures are successfully machined on 80-μm-thick cobalt-base elastic alloy under optimal conditions.

Keywords: Multiple wire electrodes; Machining efficiency; Slit width; Uniformity

1. INTRODUCTION

The requirements for miniaturization of various metal structures utilized ranging from microelectronics to biomedical fields keep growing. These requirements necessitate the development of manufacturing processes [1-3]. Electrochemical micro machining (EMM) is now receiving considerable attention because it enables the machining of micro-sized features with high accuracy and high aspect ratios in materials, regardless of their hardness and stiffness [4-6].

Micro wire EMM is a method of using micrometer scale wire as a tool cathode because it does not wear out the tool [7], which is an issue in the fabrication of metal micro parts or devices, by moving the wire electrode along a programmed path. Kim et al. first proposed a method of wire

electrochemical micro machining (WEMM) on stainless steel with a platinum electrode and obtained the micro structure with a slit width of approximately 20 μm [8]. Zhu et al. developed a micro wire electrochemical cutting process and studied the effects of process parameters on the wire diameter in the wire etching and on the gap variation in the electrochemical cutting, both theoretically and experimentally. A series of complex micro structures with a slit width of 20 μm was fabricated on a 100-μm-thick nickel plate at a feed rate of 0.125 μm/s [9]. Shin et al. investigated changes in the side gap according to the applied pulse voltage, pulse on-time and pulse period, and fabricated micro features such as micro grooves and gears in stainless steel plates at a feed rate of 0.1 μm/s [10]. To improve processing stability, Wang et al. developed a WEMM system with an axial electrolyte flow unit. High-aspect-ratio micro splines and curved flow channels with slit widths of 160 μm were fabricated on 5-mm-thick stainless steel (0Cr18Ni9) at a feed rate of 0.5 μm/s [11]. Although the machining rate was much improved, the side gap increased to more than 60 μm. Qu et al. integrated pulse electrochemical machining and a reciprocated traveling wire electrode to improve the homogeneity of slits. Wire traveling is capable of producing micro structures with feature heights up to 10 mm and aspect ratios of 50 or more [12]. However, thick wire must be used to avoid wire breakage, and direct current used as the power of the ultra-short voltage pulses is not enough. These lead to a relatively large cutting slit width. For fabricating micro structures with high-precision features, low-frequency and small-amplitude vibration of the cathode wire was adopted by Zeng et al. [13].

In order to improve the accuracy in micro wire EMM, a narrow machining gap is preferred [14]. However, a narrow machining gap limits the efficiency of mass transport and productivity. In order to improve productivity, methods for enhancing mass transport were proposed to improve the feed rate when using a single wire electrode. Zou et al. proposed a method for in situ fabricating ribbed wire electrodes and feeding rate of 1 μm/s was obtained [15]. Fang et al. adopted a rotary helical electrode and the achievable maximum electrode feed rate was increased to 7 μm s^{-1} [16]. However, the electrodes sizes in the two studies mentioned above are large and slits widths machined are in hundreds micro meter scale, which are not applicative in process using wire electrode with 10μm diameter or less.

In the present study, multiple wire electrodes with diameters of 10 μm are first introduced to improve the machining efficiency for fabricating micro structures with high-precision features. Compared with other methods, productivity can be increased by using several wire electrodes and machining several features simultaneously. The effects of the number of wire electrodes on feed rate and overall efficiency are studied, and the uniformity of the slit widths according to the applied pulse voltage, pulse on-time, pulse period and feed rate are investigated. Ultimately, structures with good uniformity in slit width is fabricated.

2. PROCESSING MODEL ANALYSIS

As shown in Figure 1, multiple wire electrode electrochemical micro machining is a method for fabricating several metal micro slits or structures simultaneously. It uses arranged wire electrodes according to certain rules. During the machining process, an appropriate voltage is applied between the

workpiece and the wire electrodes. At the anodic workpiece surface, metal is dissolved into metallic ions by electrochemical reactions.

If one of the wire electrodes is short-circuited, the machining process should be suspended, and all the wire electrodes must respond quickly. To guarantee the stability of the multiple wire electrode electrochemical micro machining process, the machining gap of each wire electrode machining branch must be controlled over a reasonable range.

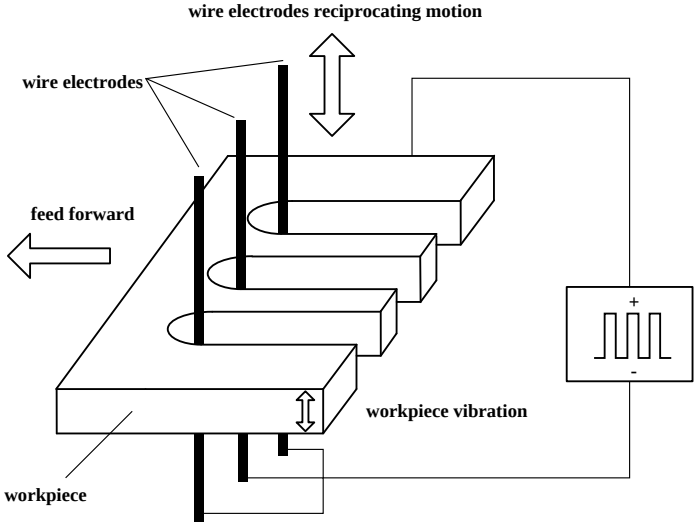

Figure 1. Schematic view of multiple wire electrode electrochemical micro machining

When multiple wire electrode electrochemical micro machining is performed with an ultra-short pulse voltage, the electrochemical process cannot achieve stationary conditions. Inductance effects cannot be disregarded in an actual system because of the very high pulse frequency. The feeder inductance represents the dominating factor during impulse distortion. In particular, for short impulses of less than 1 μs duration, the inductance is in the nanoHenry range [17]. Electrolyte resistance, inductance and electrical double layers can provide an equivalent RCL circuit in an electrochemical cell, as shown in Figure 2, where C_d is the capacitance of the double layer, which is nothing but a parallel-plate capacitor with high capacity, R_p is the polarization resistance of the double layer, R_e is the resistance between the tool and the workpiece, L_i is the inductance of the feeder, R_u is the internal resistance of the pulse supplier, n is the number of wire electrodes, and I_t is the total current.

Because all the wire electrodes are of the same diameter and the same length in the machining area, R_{p1}, R_{p2} and R_{pn} can be considered to be approximately equal to R_p. Meanwhile, C_{d1}, C_{d2} and C_{dn} can also be considered to be approximately equal to C_d. The polarization resistance is equivalent to $1/nR_p$ and the double layer capacitance is equivalent to nC_d. The circuit can be ultimately simplified to that shown in Figure 3. The time constant τ can be determined by the equation:

$$\tau = \frac{2C_d R_p L_i}{L_i + \frac{1}{n} C_d R_p R_e + C_d R_p R_u}. \quad (1)$$

When one wire electrode is used, the time constant τ will be:

$$\tau = \frac{2C_d R_p L_i}{L_i + C_d R_p R_e + C_d R_p R_u}. \quad (2)$$

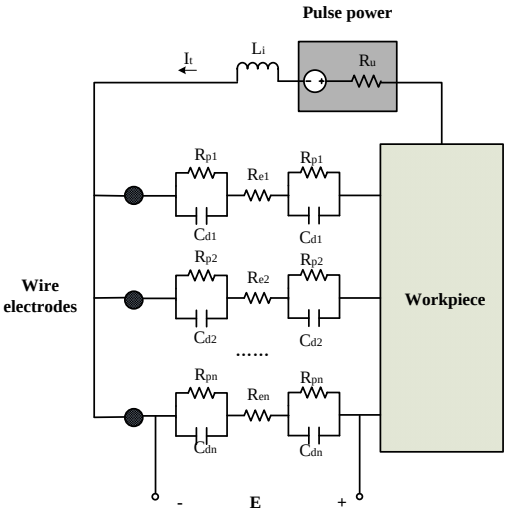

Figure 2. Equivalent circuit model for electrical double layer potential

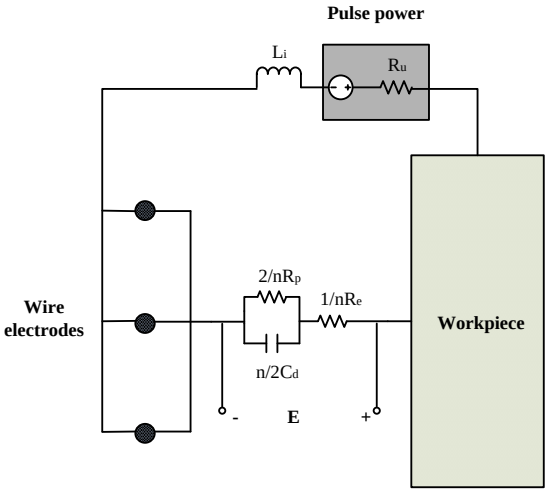

Figure 3. Simplified equivalent circuit model

From electrochemistry, after applying a voltage pulse to electrodes, transformation of electron metal conduction into ion electrolyte solution conduction in an electrical double layer can be achieved by two methods: progress of the electrochemical reaction (flow of the faradaic current) and the capacity charging current through a capacitor. The material removal acts only during the time corresponding to the faradaic currents. Thus, the amount of material removed for one pulse on-time can be determined as stated in Eq. (3) [18].

$$V_{on-time} = \int_{t*}^{\tau_{on}} \frac{CEnA}{gr} dt = nCE \int_{t*}^{\tau_{on}} \frac{A}{gr} dt = \frac{nCE\bar{A}}{\bar{g}\bar{r}} (\tau_{on} - t*) \quad (3)$$

where $V_{on\text{-}time}$ is the volume of material removed for one pulse on-time, C is the electrochemical constant, E is the voltage value acquired using an oscillograph, n is the number of wire electrodes, A is the machining area of one wire electrode, g is the inter-electrode gap, r is the electrolyte resistivity, $t*$ is the initial time of the faradaic current, which is proportional to the time constant τ, and $\bar{A}$, $\bar{g}$ and $\bar{r}$ are the average values of A, g and r. Hence, an approximation of the feed rate (FR) can be calculated as:

$$FR \cong \frac{V_{on-time}}{n\bar{A}T} = \frac{nCE\bar{A}}{n\bar{g}\bar{r}\bar{A}T} (\tau_{on} - t*) = \frac{CE}{\bar{g}\bar{r}T} (\tau_{on} - t*), \quad (4)$$

where T is the pulse period. From Eq. (4), compared with one wire electrochemical machining, there is little change in the other parameters, except for $t*$. With an increase in the number of wire electrodes, $t*$ increases as the time constant τ increases. Therefore, the feed rate will decrease with increasing number of wire electrodes. The overall machining rate (MR) can be determined as: $MR = n \times FR$.

3. EXPERIMENTAL SYSTEM

Figure 4 schematically depicts the MWEEMM experimental setup. It consists of a servo-control feed unit, a pulsed power source, an oscillograph, a piezoelectric ceramics (PZT) unit and a charge coupled device (CCD) camera. The servo-control feed unit is controlled by a motion control card that is interfaced with an industrial computer (IPC). The pulsed power source and the oscillograph are used as the signal source and the signal monitor. The electrolyte cell, which is connected to the workpiece, is positioned on a vibration table driven by the PZT controller, which produces low-frequency vibrations to enhance mass transport. The CCD camera visualizes the machining area. No circulation system is integrated during experimentation as the multiple wire electrode electrochemical micro machining process involves negligible heat generation and the amount of precipitation is very small.

Experiments are performed at room temperature. Diluted hydrochloric acid at a concentration of 0.01 M is used as an electrolyte, which is suitable for the machining of elastic alloy with a good surface finish. The workpiece is a cobalt-base elastic alloy with a thickness of 80 μm. Tungsten wire of 10 μm diameter, which is insulated with silica gel except in the machining area, is used as the tool electrodes.

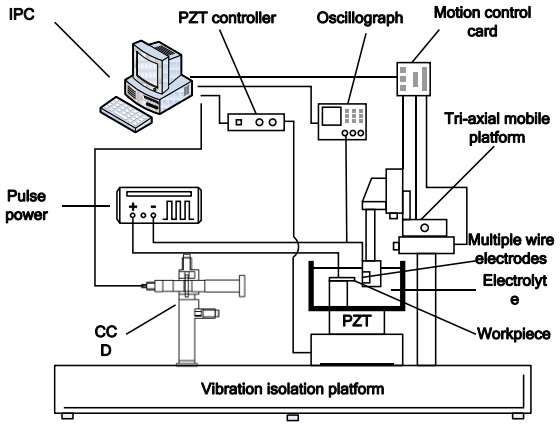

Figure 4. Schematic diagram of the experimental setup

4. RESULTS AND DISCUSSION

4.1 Effects of Number of Wire Electrodes

Figure 5 exhibits the influence of the number of wire electrodes on the machining rate. From Figure 5, when the same pulse on-time is applied, the feed rate decreases with increasing number of wire electrodes. When the number of tool electrodes increases, the cell impedance decreases because the polarization resistance decreases and the double layer capacitance increases according to the simplified circuit shown in Figure 3. The decrease of cell impedance will cause more power losses at Li and Ru. The rise time of the double layer potential will be longer because the time constant τ becomes larger according to Eq. (1). The potential may not rise sufficiently within the short pulse duration. The initial time of the faradaic current t* becomes larger because it is proportional to the time constant τ, and so $(\tau_{on}-t^*)$ will decrease. Thus, the feed rate will decrease with increasing number of wire electrodes according to Eq. (4).

The overall machining rate can be determined as: $MR=n\times FR$. As the feed rate is not constant, and decreases with increasing number of wire electrodes, the overall machining rate is not linearly related to the number of wire electrodes. From Figure 5, the maximum machining rates for one wire electrode and three wire electrodes are approximately 0.7 μm/s and 0.45 μm/s, respectively. The overall machining efficiency of three wire electrode machining increases by nearly 100% of that of one wire electrode. Hence, applying multiple wire electrodes proves to be an effective method for increasing the machining efficiency.

The minimum pulse on-time required to overcome the effects associated with a double layer capacitor is shown in Figure 6. When a 40 ns pulse on-time voltage is applied to more than five wire electrodes, machining is almost impossible because a longer pulse on-time is required. The faradaic current only starts flowing through the cell when the electrical double layer is sufficiently charged. Put another way, the double layer potential should reach the dissolution potential of the workpiece. As shown in Figure 6, the minimum pulse-on time increases with increasing number of wire electrodes. As analyzed above, the rise time of the double layer potential will be longer with a higher number of

wire electrodes. Therefore, when the feed rates are the same, a greater number of tool electrodes requires longer pulse on-times for successful machining. Park et al. also demonstrated that longer pulse on-times is necessary when the electrode size is larger [19].

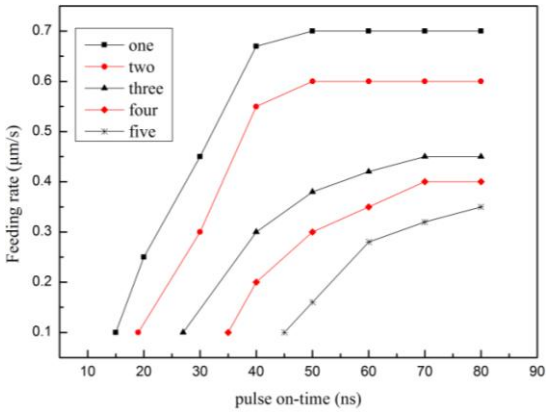

Figure 5. Feed rates according to pulse on-time and number of wire electrodes (applied voltage: 6 V, pulse period: 6 μs)

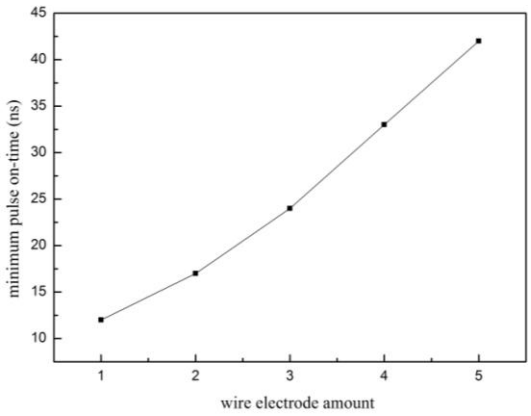

Figure 6. Minimum pulse ontime (three wire electrodes, applied voltage: 6 V, pulse period: 6 μs, feed rate: 0.1 μm/s)

4.2 Effects of Machining Conditions on Machining Accuracy

When multiple wire electrodes are used, the machining accuracy is represented by the average slit width and the uniformity of the slit widths. To investigate the effects of machining conditions on machining accuracy, comparative experiments are carried out using three wire electrodes. The uniformity of the slit width is measured using the standard deviation of three slits. The average slit width s and the standard deviation σ , as shown in Figure 7, are defined as follows:

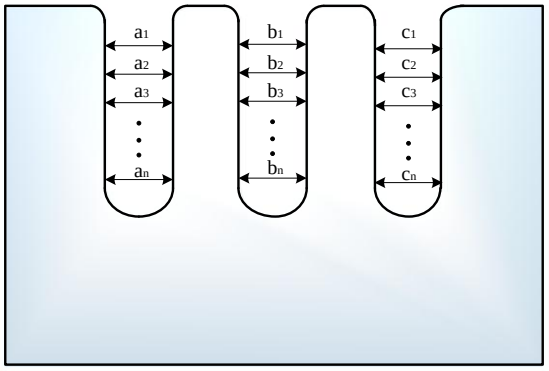

Figure 7. Schematic view of the slit widths

$$s_1 = \frac{1}{n}\sum_{i=1}^{n} a_i \quad s_2 = \frac{1}{n}\sum_{i=1}^{n} b_i \quad s_3 = \frac{1}{n}\sum_{i=1}^{n} c_i \tag{5}$$

$$s = \frac{1}{3}(s_1 + s_2 + s_3) \tag{6}$$

$$\sigma = \sqrt{\frac{\sum_{k=1}^{3}(s_k - s)^2}{3-1}} \tag{7}$$

where a_i, b_i and c_i are the measured widths of the machined slits, and s_1, s_2 and s_3 are the slit widths of slit one, slit two and slit three; n = 7 in this study.

4.2.1 Effects of Applied Voltage on Machining Accuracy

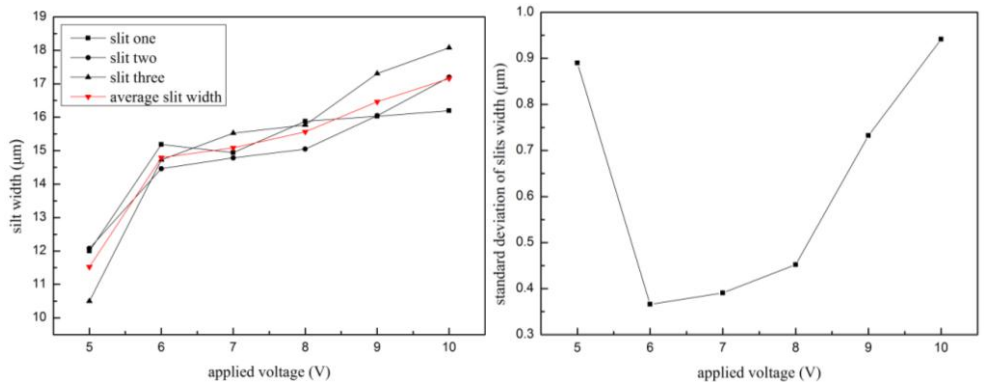

Figure 8. Effect of applied voltage on (a) slit width and (b) standard deviation of slit width (three wire electrodes, pulse period: 6 μs, pulse on-time: 40 ns, feed rate: 0.1 μm/s)

Figure 8 shows the effects of the applied voltage on each slit width, the standard deviation of the three slit widths and the average slit width, which was obtained with three wire electrodes at a pulse period of 6 μs, a pulse on-time of 40 ns and a feed rate of 0.1 μm/s. Figure 8(a) and 8(b) indicate that the uniformity of the slit widths increases with the applied voltage in the voltage range from 5 to 6

V; then, the uniformity of the slit widths decreases with a further increase of the applied voltage from 6 to 10 V. Although the width of each slit does not display a strictly increasing trend with applied voltage, the average slit width increases with the applied voltage, as shown in Figure 8(a), which is similar to the work using a single wire electrode by Lei et al. [20]. Therefore, when the applied voltage is 6 V, the uniformity of the slit widths is the best, as shown in Figure 9.

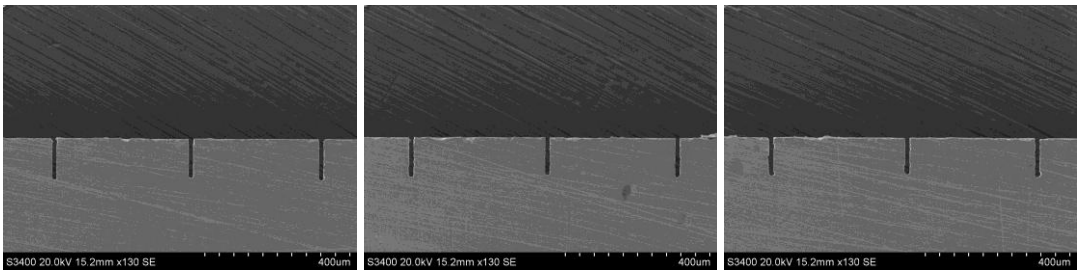

Figure 9. Micro slits with different applied voltages (a: 6 V, b: 8 V, c: 10 V)

4.2.2 Effects of Pulse On-time on Machining Accuracy

Figure 10 exhibits the effects of the pulse on-time on each slit width, the standard deviation of the three slit widths and the average slit width. From Figure 10(b), it can be seen that the standard deviation of the slit widths increases with pulse on-time. Put another way, the uniformity of the slit widths decreases with increasing pulse on-time. As shown in Figure 10(a), the average slit width increases with the pulse on-time. Qu et al. also demonstrated that a small pulse on-time leads to a tiny slit when using a single wire electrode [14]. Hence, when the pulse period is 6 μs and the feed rate is 0.1 μm/s, a pulse on-time of 30 ns is optimal for the machining process, as shown in Figure 11.

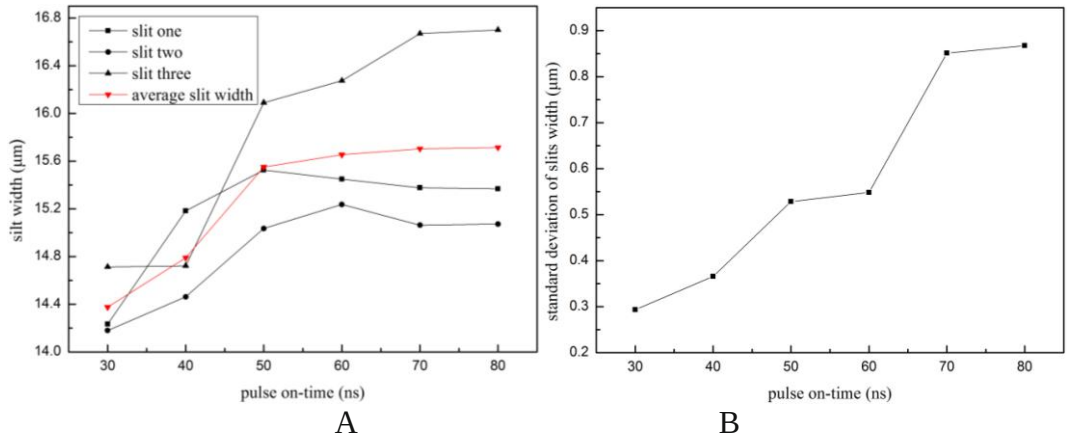

Figure 10. Effect of pulse on-time on (a) slit width and (b) standard deviation of slit width (three wire electrodes, pulse period: 6 μs, applied voltage: 6 V, feed rate: 0.1 μm/s)

Although the increase of pulse on-time can increase the faradaic current and the metal electrochemical dissolution volume, the removal of the products near the anode in the machining gap becomes difficult. Electrolytic product accumulation increases the probability of large fluctuations of electrolyte conductivity, leading to a reduction in the uniformity of the slit widths.

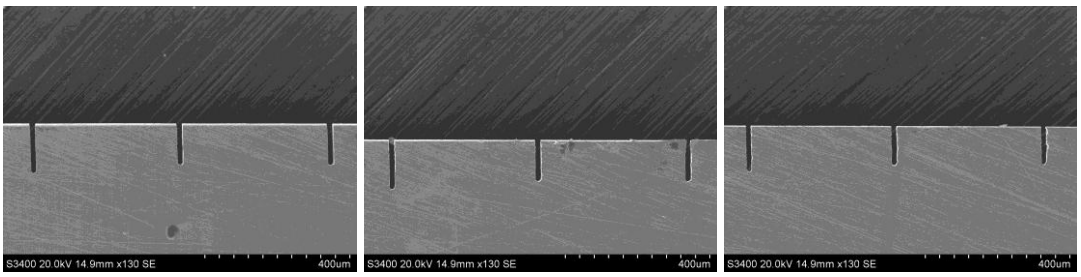

Figure 11. Micro slits with different pulse on-times (a: 30 ns, b: 50 ns, c: 70 ns)

4.2.3 Effects of Pulse Period on Machining Accuracy

The influence of the pulse period on the uniformity of the slit widths is illustrated in Figure 12. When the pulse period is 7 μs, the uniformity of the slit widths is the best, as shown in Figure 13. When the pulse on-time is a constant, for each pulse, almost the same amount of bubbles are generated. In a short pulse period, the pulse off-time is short. Therefore, the overflow time of small bubbles is shorter, and small bubbles easily accumulate between the wire and the workpiece. When the size of the accumulated bubbles increases, the wire can be deformed due to the surface tension of the bubbles. Moreover, the bubbles prevent ion diffusion or flushing of the electrolyte, which produces irregular shapes. When the pulse period is greater than 7 μs, the stability of the machining process deteriorates slightly. Shin et al. also reported that the side gap decreases as the pulse period increases [10].

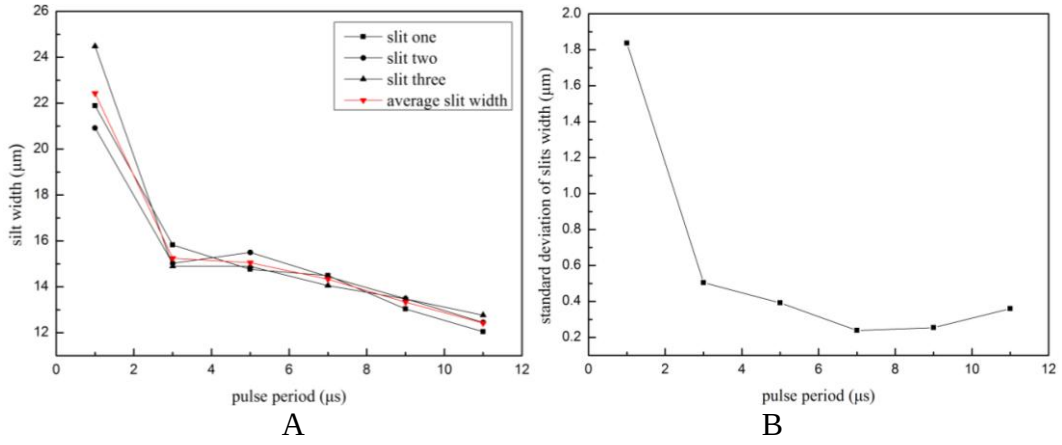

Figure 12. Effect of pulse period on (a) slit width and (b) standard deviation of slit width (three wire electrodes, pulse on-time: 40 ns, applied voltage: 6 V, feed rate: 0.1 μm/s)

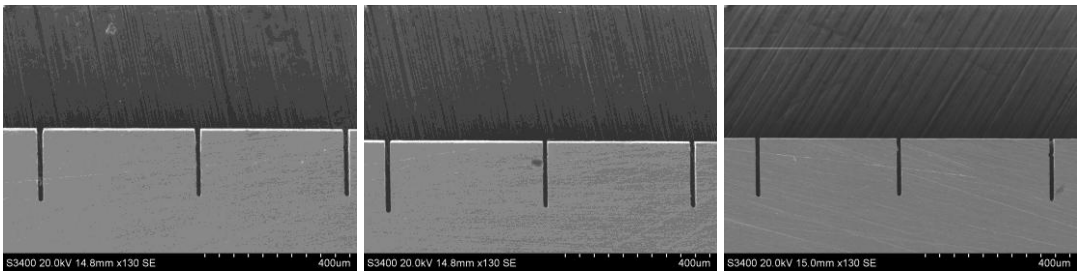

A B C

Figure 13. Micro slits with different pulse periods (a: 3 μs, b: 7 μs, c: 11 μs)

4.2.4 Effects of Feed Rate on Machining Accuracy

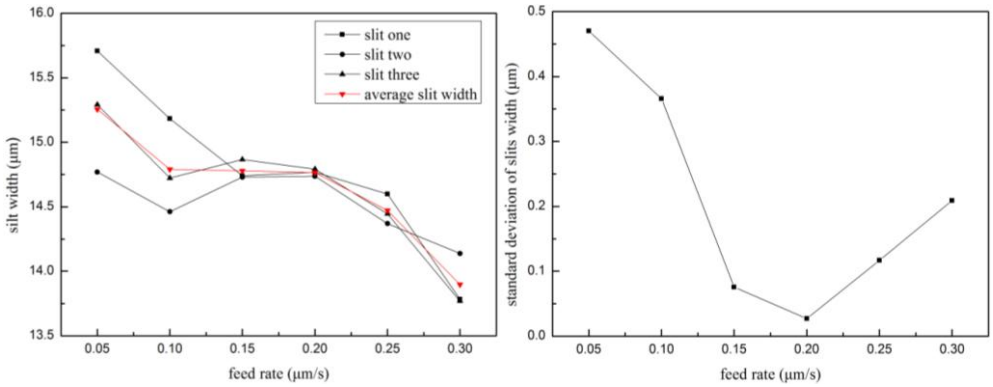

A B

Figure 14. Effect of feed rate on (a) slit width and (b) standard deviation of slit width (three wire electrodes, pulse on-time: 40 ns, applied voltage: 6 V, pulse period: 6 μs)

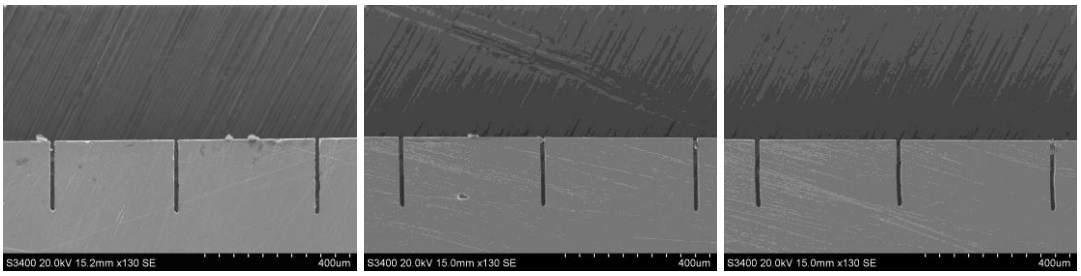

A B C

Figure 15. Micro slits with different pulse on-times (a: 30 ns, b: 50 ns, c: 70 ns)

The influence of the feed rate of the tool electrodes on the slit widths is also investigated. As shown in Figure 14, when the feed rate is 0.05 μm/s, the slit widths are relatively large and the uniformity of the slit widths is poor. For micromachining, a high tool feed rate is preferred. However, when the tool electrode feed rate is faster than 0.2 μm/s, the stability of the machining process deteriorates, as shown in Figure 15. Therefore, the optimized feed rate is set to 0.2 μm/s.

4.3 Application

Using three wire electrodes, structures were machined simultaneously on an 80-μm-thick elastic alloy plate. The machining parameters were: applied voltage of 6.0 V, pulse on-time of 40 ns, pulse period of 6 μs and feed rate of 0.2 μm/s. Figure 16 shows the fabricated micro structures; the average slit width is 14.1 μm with a standard deviation of 0.05 μm in figure 16(a), and the average slit width is 14.4 μm with a standard deviation of 0.06 μm in figure 16(b). By using three wire electrodes, three structure were obtained at the same time and the machining time was shortened compared to that using a single wire electrode.

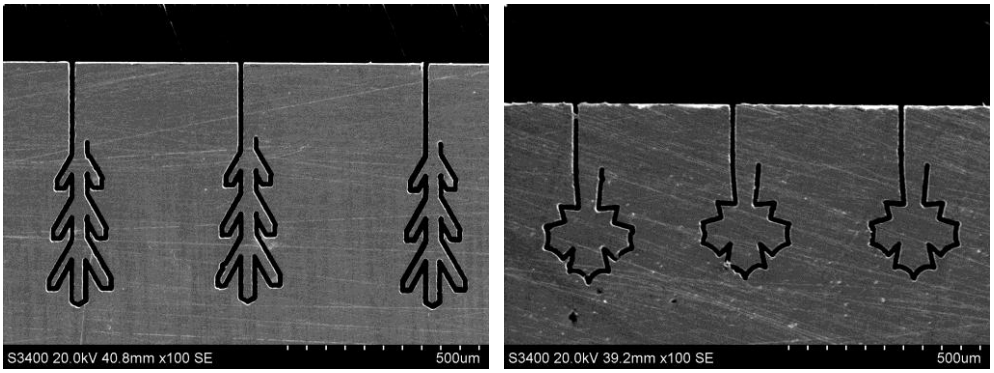

A B

Figure 16. Micro structure machined using three wire electrodes

6. CONCLUSIONS

In this paper, multiple wire electrodes have been introduced in order to increase productivity over a single micro wire electrode. Based on the experimental results, the following conclusions can be drawn:

(1) The overall machining efficiency can be increased by using multiple wire electrodes rather than a single wire electrode. However, the overall machining efficiency does not increase linearly with the number of wire electrodes.

(2) Experiments have verified that with an optimal applied voltage, pulse on-time, pulse period and appropriate feed rate, the machining accuracy can be improved.

(3) Micro structures were fabricated by three wire electrodes on an elastic alloy plate measuring 80 μm in thickness, and the machining time was shortened compared to that using a single wire electrode.

ACKNOWLEDGMENTS
This work was conducted under the sponsorship of the National Natural Science Foundation of China (51375238), the Jiangsu Natural Science Foundation (BK2013136，the Funding of Jiangsu Innovation Program for Graduate Education (CXZZ13_0153) and a project funded by the China Postdoctoral Science Foundation (2015T80546).

References

1. A. Kamaraj, M. Sundaram, and R. Mathew, *Microsyst. Technol.*, 19 (2013) 179-186.
2. M. Datta and D. Landolt, *Electrochim. Acta*, 45 (2000) 2535-2558.
3. A. Spieser and A. Ivanov, *Int. J. Adv. Manuf. Technol.*, 69 (2013) 563-581.
4. D. Chung, S. Hong, S. Min, H. Bo and N. Chong, *Int. J. Precis. Eng. Manuf.*, 12 (2011) 371-380.
5. I. Yang, S. Min and C. Chu, *Int. J. Precis. Eng. Manuf.*, 10 (2009) 5-10.
6. J. Byun, S. Hong, H. Min, H. Bo and N. Chong, *Int. J. Precis. Eng. Manuf.*, 11 (2010) 747-753.
7. C. Na, B. Park, B. Kim, D. Choi and C. Chu, *J. Korean Soc. Prec. Eng.*, 22 (2005) 37-44.
8. B. Kim, C. Na, Y. Lee, D. Choi and C. Chu, *CIRP Annals-Manuf. Technol.*, 54 (2005) 191-194.
9. D. Zhu, K. Wang and N. Qu, *CIRP Annals-Manuf. Technol.*, 56 (2007) 241-244.
10. H. Shin, B. Kim and C. Chu, *J. Micromech. Microeng.*, 18 (2008) 1-6.
11. S. Wang, Y. Zeng, Y. Liu and D. Zhu, *Int. J. Adv. Manuf. Technol.*, 63 (2011) 25-32.
12. N. Qu, H. Ji and Y. Zeng, *Int. J. Adv. Manuf. Technol.*, 72 (2014) 677-683.
13. Y.Zeng, Q. Yu, S. Wang and D. Zhu, *CIRP Annals-Manuf. Technol.*, 61 (2012) 195-198.
14. N. Qu, K. Xu, Y. Zeng and Q. Yu, *Int. J. Electrochem. Sci.*, 8 (2013) 12163-12171.
15. X. Fang, X. Zou, P. Zhang, Y. Zeng and N. Qu, *Int. J. Adv. Manuf. Technol.*, (2015) 1-11.
16. X. Zou, X. Fang, Y. Zeng, P. Zhang and D. Zhu, *Int. J. Electrochem. Sci.*, 11 (2016) 2335-2344
17. St. Burkert, H. Schulze, Th. Gmelin and M. Leone, *Int. J. Mater. Form.*, 2 (2009) 645-648.
18. M. Mithu, G. Fantoni and J. Ciampi, *Int. J. Adv. Manuf. Technol.*, 55 (2011) 921-933.
19. B. Park, B. Kim, C. Chu. *CIRP Annals-Manuf. Technol.*, 55 (2006) 197-200.
20. J. Lei, X. Wu, B. Wu, B. Xu, D. Guo, J. Zhong, *Procedia CIRP*, 42 (2016) 825-830.

© 2016 The Authors. Published by ESG (www.electrochemsci.org). This article is an open access article distributed under the terms and conditions of the Creative Commons Attribution license (http://creativecommons.org/licenses/by/4.0/).